
Fine-Grained Uncertainty Quantification via Collisions

Jesse Friedbaum¹

Sudarshan Adiga²

Ravi Tandon^{1,2}

Abstract

We propose a new approach for fine-grained uncertainty quantification (UQ) using a collision matrix. For a classification problem involving K classes, the $K \times K$ collision matrix S measures the inherent (aleatoric) difficulty in distinguishing between each pair of classes. In contrast to existing UQ methods, the collision matrix gives a much more detailed picture of the difficulty of classification. We discuss several possible downstream applications of the collision matrix, establish its fundamental mathematical properties, as well as show its relationship with existing UQ methods, including the Bayes error rate. We also address the new problem of estimating the collision matrix using one-hot labeled data. We propose a series of innovative techniques to estimate S . First, we learn a contrastive binary classifier which takes two inputs and determines if they belong to the same class. We then show that this contrastive classifier (which is PAC learnable) can be used to reliably estimate the Gramian matrix of S , defined as $G = S^T S$. Finally, we show that under very mild assumptions, G can be used to uniquely recover S , a new result on stochastic matrices which could be of independent interest. Experimental results are also presented to validate our methods on several datasets.

1 Introduction

As machine learning is applied in high risk and high uncertainty scenarios such as healthcare (Alanazi, 2022) and finance (Aziz et al., 2022), greater interest has grown around the field of classification *un-*

certainty quantification (UQ), which attempts to describe the uncertainty involved in a prediction task. UQ techniques have been developed to measure a variety of distinct phenomena using many different metrics (See Figure 1(B)). We propose a new uncertainty measurement, the *Collision Matrix*, which describes uncertainty through the probability of *class collisions*, defined as the same input value belonging to different classes when observed multiple times. An example of a class collision in healthcare would be two patients that arrive at a hospital complaining of identical symptoms (the input) such as muscle weakness, tingling in the extremities, and blurred vision, but where the symptoms are caused by different diseases (the class) such as Multiple Sclerosis and a Vitamin B12 deficiency. The prevalence of class collision between any two classes provides an intuitive characterization of how difficult it is to distinguish between that pair of classes, and the collision matrix contains the rate of collision collision rate between classes i and j in its i, j^{th} entry. In Figure 1 A, we provide an example of a 3 class setting where two classes are easily confused and one is not. The collision matrix identifies which pair of classes has uncertainty between them, whereas less detailed UQ measures such as the BER only indicate that there is uncertainty somewhere in the system.

Motivation for fine-grained UQ. This ability to quantify uncertainty between pairs of classes makes the collision matrix a uniquely fine-grained UQ technique and allows for new applications not available to less detailed UQ descriptions. For example, the collision matrix can be used to predict how the difficulty of a classification scenario will be affected by combining different classes together. This has the potential to make a previously impossible classification problem tractable. Returning to our healthcare example, it may not be possible to accurately predict the disease from a patient's initial symptoms alone, but the collision matrix could inform the creation of broader disease categories that can be predicted with high accuracy. Another application of this fine-grained uncertainty measure is to inform online changes to the cost function or sampling during training: if it is observed during training that the classifier is very likely to confuse two classes

¹Program in Applied Mathematics, University of Arizona, Tucson, AZ, USA ² Department of Electrical and Computer Engineering, University of Arizona, Tucson, AZ, USA. Correspondence to: Jesse Friedbaum (friedbaum@arizona.edu), Ravi Tandon (tandonr@arizona.edu).

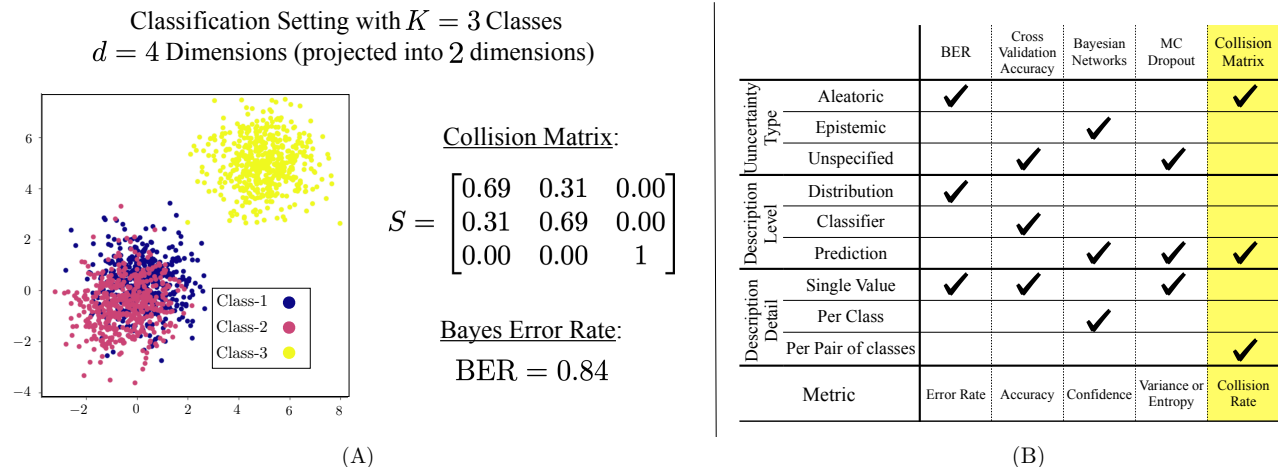


Figure 1: Part (A) shows the collision matrix (S) for a $K = 3$ class classification setting where classes 1 and 2 are easily confused with each other, but class 3 is not. This information is encapsulated in the collision matrix by the values in position 1, 2 and 2, 1 being larger than the other off-diagonal elements, but this information is not found in the BER. Part (B) compares the collision matrix against uncertainty quantification (UQ) measures BER (Tumer and Ghosh, 2003), Bayesian Networks (Ben-Gal, 2008) and MC Dropout (Folgot et al., 2021).

despite there being relatively low uncertainty between these two classes, we could increase the output on the loss function for this error or over-sample from those two classes. In this way the collision matrix does not only indicate how well a classifier has learned a data distribution, but can also indicate how a classifier can be improved.

To understand how our method relates to other UQ techniques, we next discuss how UQ techniques can be categorized and how the collision matrix fits into these categorizations (see Figure 1 A).

a) Uncertainty Type: Uncertainties involved with classification can be broadly divided into two types: *epistemic* and *aleatoric* (Hüllermeier and Waegeman, 2021). Epistemic means relating to knowledge and describes the uncertainty resulting from a lack of knowledge such as insufficient training data or a lack of knowledge about the best model parameters. For example, Bayesian Networks (Nannapaneni et al., 2016) seek model uncertainty in the choice of model parameters which is epistemic. Aleatory refers to chance and describes the uncertainty that cannot be reduced with more knowledge. For example, the Bayes Error Rate or BER (Murty and Devi, 2011) is a measure of aleatoric uncertainty because it refers to the unavoidable error even with access to the best possible classifier. The collision matrix also measures the uncertainty inherent to a data distribution making it a property of the distribution itself independent of any classifier.

b) Description Metric: In addition to describing different types of uncertainty, different UQ techniques also use a variety of metrics to measure uncertainty. Some of these metrics are very intuitive such as percent confidence or expected error rate, while other measures are

more esoteric such as Shannon Entropy (Burkhardt et al., 2018), the expected affect on a cost function (Sale et al., 2024) or the cardinality of a prediction set (Angelopoulos and Bates, 2022). We propose the new and intuitive measure: the expectation that multiple observations of the exact same input values will be found in different classes. When this expectation is large it means uncertainty is very high and no classifier could achieve high accuracy. On the other hand when this expectation is zero it means there is no inherent uncertainty at all—the setting is deterministic.

c) Description Level: A UQ measure may describe the uncertainty related to the data distribution itself (such as BER) or the uncertainty related to a particular classifier (such as the familiar cross-validation accuracy or confusion matrix) or even for an individual prediction such as the techniques presented by Harper and Southern (2020). Similar to the BER, the collision matrix describes the uncertainty arising from the distribution itself and not a specific classifier or prediction. Such measures can be used as an objective standard against which to judge the effectiveness of any classifier.

d) Description Detail: Some UQ techniques condense all uncertainty into a single value such as the BER or entropy (Burkhardt et al., 2018). Other methods such as (Sale et al., 2024) provide a more detailed description by providing uncertainty values for each class. The collision matrix provides even more detail by describing uncertainty between each pair of classes. This level of detail is one of the key advantages of measuring uncertainty with the collision matrix and allows for a fine-grained evaluation of classifier performance. Because the collision matrix is a property of the data distribution, these uncertainties can be interpreted

as measuring the similarity between pairs of classes.

Deriving further insights from the Collision Matrix. In a K -class setting the collision matrix will be a $K \times K$ matrix. The (i, j) th entry of this matrix describes the difficulty of distinguishing elements of class j from class i , which can be thought of as a measure of uncertainty or an indication of similarity between those classes. (See an example in Figure 1 A.) Elements of the collision matrix can also be combined to create less fine grained measures of uncertainty as illustrated in Figure 2. For instance, the i th column of the collision matrix indicates the difficulty of avoiding false negative classifications when the true class is i indicative of the achievable recall on class i . On the other hand, the i th row describes how difficult it is to avoid false positive classifications into class i related to the possible precision. Finally, the diagonal elements of the collision matrix can be used to find a single value measure of the overall uncertainty in \mathcal{D} related to the BER. More details in Section 2.2 and Figure 2.

Summary of Contributions: In Section 2, we rigorously define a novel UQ measure, the collision matrix, as a stochastic matrix comprised of the class collisions rates between individual pairs of classes. We also show how it can also be defined using the pdfs describing the data distribution. Additionally, we show how the collision matrix can be interpreted as the expected confusion matrix of a *Probabilistic Bayes Classifier* which is closely related to the *Bayes Optimal Classifier*, drawing a close link between the collision matrix and the BER. In Section 3, we examine the problem of estimating the collision matrix and develop an estimation method that takes advantage of the unique mathematical properties of the collision matrix. Specifically we show that under mild conditions the collision matrix (and all stochastic matrices) is uniquely defined by its Grammian Matrix G . We then show how G can be approximated using a PAC learnable pair-wise comparison classifier. Finally, in Section 4 we perform numerical evaluations of our method on synthetic and real world data sets. We also estimate the collision matrix directly by using calibrated networks, MC dropout and Bayesian networks. Our results show that our Grammian based method provides better estimates of the collision matrix. Finally, we consider four real world datasets and show the new/additional insights that one can draw from the collision matrix.

2 The Collision Matrix

2.1 Definition of the Collision Matrix

We define our setting by assuming that we are given training data $\mathcal{T} = \{(\mathbf{x}^{(i)}, c^{(i)})\}_{i=1}^n$ sampled i.i.d. from an unknown distribution \mathcal{D} over ordered pairs

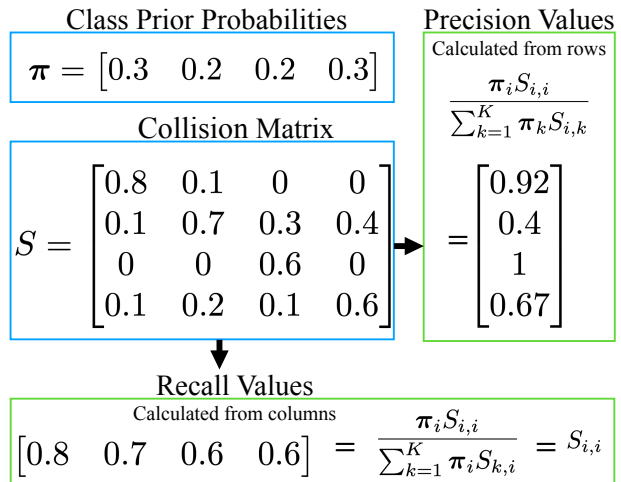


Figure 2: Using the collision matrix (S) and class prior probabilities ($\pi_{k,s}$) to calculate class precision and recall values (see Section 2.2 for further discussion.)

(\mathbf{x}, c) . Here \mathbf{x} represents a d dimensional *feature vector*, $\mathbf{x} \in \mathcal{X} \subset \mathbb{R}^d$. The label c indicates to which of K classes \mathbf{x} belongs, $c \in \{1, 2, \dots, K\}$. To further describe \mathcal{D} , we use π describe the class prior probabilities, $\pi_k = \mathbb{P}_{\mathcal{D}}(c = k)$. The conditional distribution of feature vectors in \mathcal{D} , given that the class $c = k$ is known, is denoted \mathcal{D}_k with corresponding pdf $f_k(\cdot)$. An object of key importance for understanding uncertainty in a data distribution is the posterior class probability distribution of a feature vector \mathbf{x} .

Definition 2.1 (Posterior Class Probability Distribution) *The posterior class probability distribution of a feature vector \mathbf{x} is defined as*

$$\mathbf{y}(\mathbf{x}) = (\mathbb{P}_{\mathcal{D}}(c = 1|\mathbf{x}), \dots, \mathbb{P}_{\mathcal{D}}(c = k|\mathbf{x})). \quad (1)$$

In general $\mathbf{y}(\mathbf{x})$ can be any element of the K -simplex, written as \mathcal{K} . One important special case is when all $\mathbf{y}(\mathbf{x})$ are *one-hot*, meaning $y_i(\mathbf{x}) = 1$ for some $1 \leq i \leq K$, and $y_k(\mathbf{x}) = 0$ for $k \neq i$. In this case the label is deterministically defined by the feature vector and there is no aleatoric uncertainty in \mathcal{D} (even if individual classifiers may be uncertain in their predictions). The further from one-hot these posterior distributions are, the more uncertainty is found in \mathcal{D} . Estimating these posterior distributions is very difficult, and we describe uncertainty through class collisions.

Definition 2.2 (Class Collision) *A class collision occurs when (\mathbf{x}, c) and $(\tilde{\mathbf{x}}, \tilde{c})$ are drawn from \mathcal{D} such that $\mathbf{x} = \tilde{\mathbf{x}}$ but $c \neq \tilde{c}$.*

Similar to the class posterior distributions, class collisions can directly indicate whether there is aleatoric uncertainty in a distribution: a distribution \mathcal{D} has aleatoric uncertainty if and only if class collisions are

possible. As the likelihood of class collision increases there is more uncertainty in the distribution, however, the probability of directly observing a class collision, defined by $\mathbb{E}_{(\mathbf{x},c)\sim\mathcal{D}}[\mathbb{E}_{(\tilde{\mathbf{x}},\tilde{c})\sim\mathcal{D}}[\mathbb{P}(\mathbf{x} = \tilde{\mathbf{x}}, c \neq \tilde{c})]]$, is not a good measure of uncertainty. This is because the odds of ever observing identical inputs in a large feature space \mathcal{X} are almost zero. For example, if a hospital collects variety of information on a new patient (age, height, weight, blood pressure, etc.), it is very unlikely that two patients will ever completely have identical features. This does not mean, however, that there is little uncertainty in the setting; patient intake data may not be enough to identify a disease with certainty. For this reason, we use the probability of a collision given that a feature vector has already been observed twice. We partition these probabilities based off of which class the input was observed in its first and second appearance to get K^2 values which we organize these values into the *collision matrix*.

Definition 2.3 (Collision Matrix) *The collision matrix S is a column stochastic matrix defined by*

$$S_{i,j} = \mathbb{E}_{\mathbf{x}\sim\mathcal{D}_j} \mathbb{P}(c = i|\mathbf{x}). \quad (2)$$

Each $S_{i,j}$ represents the expectation that a feature vector which was previously observed in class j will be found in class i if it is observed again, resulting in a class collision.

We now present a couple of examples of what the collision matrix S could represent in a specific applications. In our disease diagnosis example, $S_{i,j}$ represents the probability that a patient with the same features as a patient with disease j will actually have disease i . This value indicates how difficult it is to distinguish between the two disease. For a second example, suppose a university gives incoming students a survey about their personality and interests. The responses to the survey are used as feature vectors with the class corresponding to the major from which the student graduates. In this example the $S_{i,j}$ represents how often we would expect a student, whose survey answers are identical to a student who graduated in major j , to end up graduating from major i . This could be interpreted as indicating the inherent difficulty in predicting between those majors or, alternatively, a measure of how similar majors i and j are based off of the similarity of the students in each major.

2.2 Relation to the BER

We noted in the introduction that the collision matrix is similar to the BER in purpose: both describe the aleatoric uncertainty of the entire distribution \mathcal{D} . We show how the S can further be related to the BER leading to new interpretations of the collision matrix. The

Bayes Optimal Classifier is the classifier that achieves the best possible accuracy of any classifier.

Definition 2.4 (Bayes Optimal Classifier) *The Bayes Optimal Classifier $M_{opt} : \mathcal{X} \rightarrow \{1, 2, \dots, k\}$ always outputs the most likely class*

$$M_{opt}(\mathbf{x}) = \arg \max(\mathbf{y}(\mathbf{x})). \quad (3)$$

The BER is simply the error rate of this classifier. To link this to the collision matrix we define the closely related *Probabilistic Bayes Classifier* (PBC).

Definition 2.5 (Probabilistic Bayes Classifier) *The Probabilistic Bayes Classifier (PBC) $M_{prob} : \mathcal{X} \rightarrow \{1, 2, \dots, k\}$ is a non-deterministic classifier that samples its output from the posterior class probabilities*

$$M_{prob}(\mathbf{x}) \sim \mathbf{y}(\mathbf{x}). \quad (4)$$

We note that the PBC will predict the an elements of class j is in class i at a rate of $\mathbb{E}_{\mathbf{x}\sim\mathcal{D}_j} \mathbf{y}_i(\mathbf{x}) = \mathbb{E}_{\mathbf{x}\sim\mathcal{D}_j} \mathbb{P}(c = i|\mathbf{x}) = S_{i,j}$. This means that the collision matrix can be interpreted as the expected confusion matrix of the PBC. Accordingly, the off-diagonal elements in row i of S represent the rates of false positives into class i and the off-diagonal elements column i represent the false negative classification in class i . We can use the diagonal elements of S to produce a single value measure of uncertainty by finding the error rate of the PBC which we denote as the PBER. Figure 2 shows how S can be used to find precision, recall.

$$\text{PBER}(\mathcal{D}) = \sum_{k=1}^K \pi_k (1 - S_{k,k}) = 1 - \sum_{i=1}^K \pi_k S_{k,k}. \quad (5)$$

For the special case of uniform class priors, i.e., $\pi_k = 1/K$ for all k , the above expression simplifies to $\text{PBER}(\mathcal{D}) = 1 - \text{Tr}(S)/K$, where $\text{Tr}(S)$ denotes the trace of the collision matrix S .

2.3 Additional Properties and Case Study

We now examine the mathematical properties of S , which are described in Theorem 2.6. We then analyze the properties of the collision matrix in the $K = 2$ class setting to gain additional insights. The proof of Theorem 2.6 is presented in Appendix 6.2.1.

Theorem 2.6 (Properties of S) *The entries of S are defined by*

$$S_{i,j} = \mathbb{E}_{\mathbf{x}\sim\mathcal{D}_j} \mathbb{P}(C = i|\mathbf{x}) = \pi_i \int_{\mathcal{X}} \frac{f_i(\mathbf{x})f_j(\mathbf{x})}{\sum_{k=1}^K \pi_k f_k(\mathbf{x})} d\mathbf{x}. \quad (6)$$

S is a column stochastic matrix. In the special case with uniform class priors, i.e., $\pi = (\frac{1}{K}, \frac{1}{K}, \dots, \frac{1}{K})$, S is a symmetric matrix and therefore doubly stochastic.

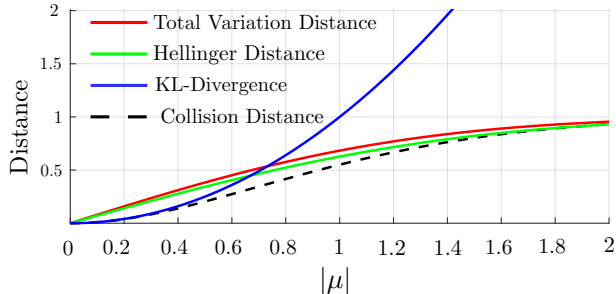


Figure 3: Comparison of $\mathcal{D}_{\text{collision}}$ (collision distance) versus other statistical distance measures for $K = 2$ classes as a function of $|\mu|$ (larger $|\mu|$ indicates larger *distance* between class distributions).

Case Study for $K = 2$ & Collision Distance. We next discuss the implications of the theorem in the simplest non-trivial case of binary classification ($K = 2$) with equal priors ($\boldsymbol{\pi} = (\frac{1}{2}, \frac{1}{2})$) which arises in several practical scenarios. In this case, the 2×2 collision matrix S is doubly stochastic and fully described by $S_{1,2}$ (off-diagonal entry) which measure the similarity of \mathcal{D}_1 and \mathcal{D}_2 . It turns out that $S_{1,2}$ takes values in the range $S_{1,2} \in [0, 1/2]$, a fact we prove in Appendix 6.2.2 using the AM-GM-HM inequality. The minimum value of $S_{12} = 0$ occurs iff \mathcal{D}_1 and \mathcal{D}_2 have disjoint support (the setting is deterministic). $S_{1,2}$ achieves a maximum of $1/2$ iff $\mathcal{D}_1 = \mathcal{D}_2$ and the posterior class probability distributions $\mathbf{y}(\mathbf{x}) = (1/2, 1/2)$ are uninformative. By shifting and re-scaling $S_{1,2}$, we can define a measure of difference between distributions as $\mathcal{D}_{\text{collision}}(\mathcal{D}_1, \mathcal{D}_2) = 1 - 2S_{1,2} \in [0, 1]$. This *collision-distance* quantifies how dissimilar two distribution are base on the likelihood of class collisions. In Figure 2.3 we compare $\mathcal{D}_{\text{collision}}$ to common statistical divergence measures for univariate Gaussian distributions $\mathcal{N}(\mu, 1)$ and $\mathcal{N}(-\mu, 1)$ as a function of μ . Remarkably, $\mathcal{D}_{\text{collision}}$ exhibits its own unique shape with two inflection points that is distinct from Total-Variation, Hellinger and KL-divergences.

3 Estimating The Collision Matrix

Baseline Approaches: We now turn our attention to estimating the collision matrix. One approach is to replace the expectation with an empirical mean in equation (2). If we partition the training data $\mathcal{T}_k = \{\mathbf{x} | (\mathbf{x}, c) \in \mathcal{T}, c = k\}$, this approach is described by

$$S_{i,j} \approx \frac{1}{|\mathcal{T}_j|} \sum_{\mathbf{x} \in \mathcal{T}_j} \mathbb{P}(c = i | \mathbf{x}) = \frac{1}{|\mathcal{T}_j|} \sum_{\mathbf{x} \in \mathcal{T}_j} \mathbf{y}_i(\mathbf{x}). \quad (7)$$

Solving (7), however, requires the class posterior probabilities $\{\mathbf{y}(\mathbf{x}^{(i)})\}_{i=1}^n$ (which are not given) and does not utilize the unique mathematical properties of S . Note that classifiers $M : \mathcal{X} \rightarrow \mathcal{K}$ are typically trained to maximize accuracy and $M(\mathbf{x})$ may not be close to $\mathbf{y}(\mathbf{x})$. It is possible to use existing UQ techniques to

improve estimates of the posterior distributions such as *calibrating* the model Guo et al. (2017) or creating a distribution of classifier outputs through *Monte Carlo (MC) Dropout* Folgoc et al. (2021) or a *Bayesian network* Ben-Gal (2008). In Section 4 we will apply these methods and equation 7 as baselines for estimating S .

We next describe a novel two step method for estimating S that avoids estimates of $\{\mathbf{y}(\mathbf{x}^{(i)})\}_{i=1}^n$ by taking advantage of the mathematical properties of S . We show that our method outperforms the baselines in Section 4.

Step 1: Estimate the Grammian $G = S^T S$

↓

Step 2: Recover S from G

Recoverability of S from G : Our two step method involves first estimating the Grammian matrix of S , defined as $G = S^T S$, and then recovering S from G . To justify this we must show that the G uniquely determines S . It is known that for any Gramian matrix G there are infinitely many matrices L satisfying $L^T L = G$ (see Lemma 6.1 in the Appendix). To the best of our knowledge, however, the specific properties of the Gramian of a stochastic matrix have not been studied. In Theorem 3.1, we provide a new theoretical result that shows that there are only finitely many invertible stochastic matrices that satisfy $L^T L = G$.

Theorem 3.1 (Uniqueness of Stochastic Gramian Factorization) *Let $G = S^T S$ be the Gramian Matrix of an invertible stochastic matrix S . Then a stochastic matrix L satisfies $L^T L = G$ if and only if $L = PS$ for some permutation matrix P .*

Intuition and proof-sketch. Theorem 3.1 tells us that, when S is invertible, G uniquely determines S up to row permutations and there are only $K!$ possible choices of S . We prove Theorem 3.1 in the Appendix 6.2.4 by showing that any two stochastic matrices S and L satisfying $S^T S = L^T L$ satisfy $L = QS$ for a Q that is both orthogonal and stochastic. We then show that such a Q must be a permutation matrix.

Theorem 3.1 reduces the uncertainty in decomposing a G , but still leaves some ambiguity in the choices of S so we must apply another constraint to S in order to ensure it is uniquely determined by G . Based on the operational interpretation of S , we choose our constraint: S should be (strictly) diagonally dominant which ensures S is invertible and limits us to a single choice of row permutation.

Corollary 3.2 *Suppose that S is a strictly diagonally dominant stochastic matrix. That is*

$$S_{j,j} > \sum_{k \neq j} S_{k,j}, \quad (8)$$

equivalent to

$$\mathbb{E}_{\mathbf{x} \sim \mathcal{D}_j} \mathbb{P}(C = j | X = \mathbf{x}) > \mathbb{E}_{\mathbf{x} \sim \mathcal{D}_j} \mathbb{P}(C \neq j | X = \mathbf{x}), \quad (9)$$

for all $k, j \in \{1, 2, \dots, K\}$. Then the Gramian Matrix G uniquely defines S .

The practical interpretation of (8) is that feature vectors drawn from the distribution of feature vectors in class j are—in expectation—more likely to be in class j than any other class. This is not necessarily true for every \mathcal{D} , especially when there are large disparities in class priors ($\pi_j \ll \pi_i$ for some i and j). We argue that this is a reasonable assumption, however, because any \mathcal{D} not following this assumption would have such great uncertainty that any prediction task is unreasonable. Specifically, when S is not diagonally dominant, even if we knew the precise distribution of the feature vectors in some class j , we would still fail to produce points in class j a majority of the time.

Estimating G using pairwise classifier: Now that we know G is sufficient to recover S we present a detailed explanation of how G may be estimated. We begin by analyzing G 's basic properties.

Definition 3.3 (Gramian of the Collision Matrix) *If S is a collision matrix, then its Gramian Matrix G is defined by $G = S^T S$. G is symmetric positive semi-definite and its elements satisfy*

$$G_{i,j} = \mathbb{E}_{\mathbf{x} \sim \mathcal{D}_i} \left[\mathbb{E}_{\tilde{\mathbf{x}} \sim \mathcal{D}_j} [\mathbb{P}(c = \tilde{c} | \mathbf{x}, \tilde{\mathbf{x}})] \right]. \quad (10)$$

Additionally, if $\boldsymbol{\pi} = (1/K, 1/K, \dots, 1/K)$, then G is doubly stochastic. We prove (10) in Appendix 6.2.3.

According to (10), $G_{i,j}$ represents that expectation that two feature vectors—one previously observed in class i and the other observed in class j —will be in the same class if observed again. This can also be seen as a measure of the similarity of class i and class j . The probability term in (10) is a measure of pairwise similarity between two inputs. In a recent work, (Friedbaum et al., 2024) studied the problem of estimating this measure in relation to the task of generating trustworthy counterfactuals. They showed that creating a pair-wise binary classifier $V(\mathbf{x}, \tilde{\mathbf{x}}) \approx \mathbb{P}(c = \tilde{c} | \mathbf{x}, \tilde{\mathbf{x}})$ via one-hot training data is a PAC learnable problem. We adopt this approach for our problem; in order to build a training dataset for learning this pair-wise binary classifier, we use the training data \mathcal{T} to create a new set of *difference training data*

$$\mathcal{T}_{\text{difference}} = \{(\mathbf{x}^{(i)}, \mathbf{x}^{(j)}), z^{(i,j)} | \mathbf{x}^{(i)}, \mathbf{x}^{(j)} \in \mathcal{T}\}, \quad (11)$$

where the new label, $z^{(i,j)} = \mathbb{1}(c^{(i)} = c^{(j)})$, indicates whether the pair belongs to the same class. Interestingly, the cardinality of the difference training data

Algorithm 1 *Collision Matrix Estimation via Gramian and Pairwise Contrast*

Step A: Train a pairwise contrastive classifier V using the difference training data defined in (11).

Step B: Use V to estimate the entries of the Gramian matrix G using (12).

Step C: Solve (14) via gradient descent to get the estimated collision matrix.

Step D: (If necessary) Permute the rows of the collision matrix to achieve diagonal dominance.

$\mathcal{T}_{\text{difference}}$ is n^2 , so this is possible even in settings with small initial training data \mathcal{T} . The first step of our algorithm is to train such a pairwise classifier V using $\mathcal{T}_{\text{difference}}$. Once V is obtained, we estimate the entries of G by replacing the expectations in (10) with the empirical averages and replacing $\mathbb{P}(c = \tilde{c} | \mathbf{x}, \tilde{\mathbf{x}})$ with $V(\mathbf{x}, \tilde{\mathbf{x}})$ to arrive at

$$\hat{G}_{i,j} \approx \frac{1}{|\mathcal{T}_i| |\mathcal{T}_j|} \sum_{\mathbf{x} \in \mathcal{T}_i} \sum_{\tilde{\mathbf{x}} \in \mathcal{T}_j} V(\mathbf{x}, \tilde{\mathbf{x}}). \quad (12)$$

Recovery of S from the estimate \hat{G} : Now that we have an estimate of G we must use it to find our estimate of S . From Corollary 3.2 we know that under reasonable assumptions our S should be uniquely defined by G , but we still need an algorithm to find S . We propose defining an optimization problem

$$\min_{\hat{S} \in \mathcal{S}} \|\hat{S}^T \hat{S} - \hat{G}\|_F, \quad (13)$$

where \mathcal{S} is the set of diagonally dominant stochastic matrices. To solve (13) we use gradient descent with an added penalization term to ensure that \hat{S} is stochastic. The penalty term includes (a) the sum of the absolute difference between column sums of \hat{S} and 1 and (b) the sum of negative values of \hat{S} :

$$\arg \min_{\hat{S}} \|\hat{S}^T \hat{S} - \hat{G}\|_F + \lambda \left(\|\hat{S}^T \mathbf{1} - \mathbf{1}\|_1 - \sum_{i=1}^K \sum_{j=1}^K \min\{\hat{S}_{i,j}, 0\} \right). \quad (14)$$

Here λ is an appropriately sized constant. Any permutation of the rows S will solve (14) so we may need to rearrange the rows of \hat{S} to ensure diagonal dominance. We present the meta algorithm (Algorithm 1) above (detailed implementation and discussion of computational complexity is provided in the Appendix 6.3.2).

4 Experiments & Discussion

In this section, we present experimental results to illustrate (a) our two-step method effectively estimates S , outperforming baselines, and (b) that the collision matrix provides useful insights into data not found by

		Scenario A			Scenario B		
Approach	Metric	Number of Classes			Amount of Class Distribution Overlap		
		$K = 3$	$K = 4$	$K = 5$	Least BER = 0.05	Medium BER = 0.11	Most BER = 0.26
Algorithm 1 (This paper)	Avg. TVD	0.0187	0.049	0.0634	0.0268	0.0463	0.0610
	Max. TVD	0.0264	0.0634	0.0913	0.0626	0.0864	0.0865
Calibrated Classifier	Avg. TVD	0.1283	0.0402	0.0711	0.0432	0.528	0.0774
	Max. TVD	0.1486	0.0691	0.1324	0.0862	0.0883	0.1507
Monte Carlo Dropout	Avg. TVD	0.1024	0.0471	0.0679	0.0642	0.1283	0.1801
	Max. TVD	0.1463	0.0718	0.1271	0.1641	0.2985	0.2772
BNN	Avg. TVD	0.0429	0.1258	0.1483	0.0048	0.0059	0.0048
	Max. TVD	0.0789	0.2508	0.2473	0.0095	0.0082	0.0078

		Training epochs →			
Approach	Metric	25 epochs	50 epochs	75 epochs	500 epochs
Algorithm 1 (This paper)	Avg. TVD	0.1083	0.1010	0.0838	0.0268
	Max. TVD	0.1743	0.1714	0.1350	0.0626
BNN	Avg. TVD	0.1034	0.1099	0.1105	0.0048
	Max. TVD	0.2338	0.3040	0.2707	0.0095

Scenario C

Figure 4: Results on Estimating S for Synthetic datasets: comparison of Gramian based approach (Algorithm 1; this paper) vs. three Baseline approaches– (1) calibrated classifier; (2) MC dropout and (3) Bayesian neural network (BNN) ensemble. Algorithm 1 outperforms the baselines in all cases in Scenario A, outperforms all but the BNN in Scenario B. We note, BNN only outperforms Algorithm 1 after very long training times (Scenario C).

other UQ methods. For part (a) to show that we can estimate S effectively we create a variety of synthetic Gaussian mixture data sets where we can calculate true posterior distributions and the ground truth S matrix. We then estimate S from sampled training data using baseline approaches and our Gramian based method. We compare the respective estimates from each method to the true S and show an advantage for the Gramian method. For part (b), to show that S provides useful insights, we estimate S on a variety of real world data sets from different fields. We use S to calculate the precision/recall values of the Probabilistic Bayes Classifier; this allows us to interpret the results in terms of what tasks may be accomplished with the data in these sets and what tasks are not possible with this data. Details on model architectures, training procedures & hyper parameters are included in Appendix 6.3. Our code is also available online¹.

Synthetic Data and Estimating S : Our synthetic data is generated using Gaussian mixtures: the feature vectors from each class are drawn from a unique multivariate normal distribution: $\mathcal{D}_k = \mathcal{N}(\boldsymbol{\mu}_k, \Sigma)$. We sample training data from these distribution to use in constructing estimates \hat{S} of the collision matrix. As described in Section 3, for baseline estimates \hat{S} we solve 7 using approximations of the posterior distribution $\mathbf{y}(\mathbf{x}^{(i)})$ from 1) a calibrated classifier, 2) an ensemble model using Monte Carlo (MC) Dropout and 4) a Bayesian Neural Network (BNN) ensemble (see de-

tails in the Appendix). We compare these baselines with our two-step Gramian based Algorithm 1. In the Gaussian mixture setting we have access to the true collision matrix S which we compare to our estimates \hat{S} the average and maximum *total variation distance* (TVD) between the columns of \hat{S} and the corresponding columns of S (recall that each column of S represents a probability distribution).

Scenario A (impact of varying number of classes).

We first report the results for relatively simple $d = 4$ dimensional data, where we increase the classification complexity by increasing K , the number of classes (Gaussian distribution in the mixture). Details of the configuration are found in the Appendix 6.3.3. We present our results in Figure 4 where the Gramian based method is the best overall method having lowest maximum TVD in all cases.

Scenario B (impact of class overlap heterogeneity).

For these tests we chose a more complicated setting with $d = 20$ dimensional data in $K = 5$ classes. We then varied the amount of uncertainty in the system by moving the data sets closer or further apart to change the amount of overlap between distributions. We report the results of these experiments in Figure 4 where we also list the BER for each configuration to demonstrate the shift in uncertainty. We report on the results where the Gramian method consistently outperforms all baselines except placing behind the BNN that performs extremely well in this high-dimension setting. We also note its comparative advantage is larger in the lower overlap settings.

¹https://anonymous.4open.science/r/Classification_Uncertainty9055/Readme

	German Credit	Adult Income	Law School	Diabetes
Collision Matrix (S)	$\begin{bmatrix} 0.655 & 0.331 \\ 0.345 & 0.669 \end{bmatrix}$	$\begin{bmatrix} 0.738 & 0.264 \\ 0.262 & 0.736 \end{bmatrix}$	$\begin{bmatrix} 0.671 & 0.299 \\ 0.329 & 0.701 \end{bmatrix}$	$\begin{bmatrix} 0.655 & 0.344 \\ 0.355 & 0.656 \end{bmatrix}$
Class Priors	$[0.3 \quad 0.7]$	$[0.761 \quad 0.239]$	$[0.159 \quad 0.841]$	$[0.888 \quad 0.112]$
Recall	$[0.665 \quad 0.656]$	$[0.738 \quad 0.736]$	$[0.671 \quad 0.701]$	$[0.655 \quad 0.669]$
Precision	$[0.453 \quad 0.820]$	$[0.899 \quad 0.463]$	$[0.221 \quad 0.944]$	$[0.913 \quad 0.268]$
Key Uncertainty Concern	Low Precision for Bad Credit: Close to half of those predicted to be a bad risk will not be credit risks.	Low Precision for High Income: Close to half of those predicted to have high income will have low income.	Low Precision for Failing in Bar: A large majority of those predicted to fail the bar will pass the bar.	Low Precision for Predicting Diabetes: A large majority of those predicted to have diabetes will not have diabetes.

Figure 5: Results and Insights provided by S for four Real-world datasets: We report the estimated collision matrix and use it to compute the recall and precision of the probabilistic Bayes classifier on these data sets. We highlight the prediction uncertainties inherent (and therefore unavoidable) in these classification problems.

Scenario C (training costs). Although the BNN performed remarkably well in Scenario B we note that it required many more training epochs to achieve better accuracy than our Algorithm 1. Considering that this is the primary computational cost of both Algorithm 1 and baseline methods (see Appendix 6.3.1), this means the Gramian based method has considerable computational benefits. We present the accuracy of the BNN baseline and The Gramian method at different points in their training in Figure 4. The Gramian method is the most well rounded method performing best on simpler classification problems (less overlap between distributions) and being more efficient to compute on complicated distributions (more overlap between distributions).

Real World Data and Insights from S : To show that S can produce useful information on real world data, we use four datasets containing the clear possibility of class collision (aleatoric uncertainty). (i) Adult income dataset (Becker and Kohavi, 1996) (Task: predict income bracket using demographic information); (ii) Law School Success dataset (Wightman, 1998) (Task: predict if a student will pass the BAR law exam from demographic & academic records); (iii) Diabetes Prediction dataset (CDC, 2015): (Task: predict if an individual is diabetic using health conditions and habits); and (iv) German Credit dataset (Hofmann, 1994): (Task: predict credit risk using loan application and demographic data).

We estimate the collision matrix using Algorithm 1 for all data sets, and then find the precision and recall for the probabilistic Bayes classifier (PBC) as described in Section 2.2 and Figure 2. We present our results in Figure 5. Unlike single value uncertainty measures, such as the BER, the collision matrix informs us exactly what types of classification problems are inevitable in the data. For example, the uncertainty and class imbalances in the adult income data set will

cause low precision for predicting high income such that a most of those predicted to have high income by the PBC will not have high income. These insights can have important practical implications: we found very low precision for diabetes (three quarters of those predicted to have diabetes will not have it), but we had much better recall with 67% of individuals with diabetes being correctly classified. These values suggest: the information in this dataset is useful for identifying individuals who are at high risk for diabetes and should undergo further testing (good recall), but the information in this data set is not sufficient to make trustworthy diagnoses (low precision). We emphasize that the collision matrix is a property of the data set, so training more sophisticated models on this dataset can not lead to high precision diagnoses, rather richer data (e.g., more informative features) could be necessary before a classifier can achieve high precision. On the other hand, if a classifier on this data set achieves recall for diabetes well below 67%, we know that it is possible to achieve better recall suggesting we adjust the classifier architecture or training procedure. This level of detail about what kind of classification performance is possible from a data set is a unique benefit of the fine-grained nature of S .

5 Conclusion

We introduced the *Collision Matrix* as a new fine-grained approach for capturing aleatoric uncertainty in classification problems. Collision matrix provides a uniquely detailed description of uncertainty, measuring the difficulty in distinguishing between pairs of classes and providing unique insights for classification tasks. We developed the fundamental properties of S ; and leveraged those to devise a novel pairwise contrastive approach for estimating S . Furthermore, we validated the effectiveness of our estimation algorithm as well as showed the kind of insights that can be drawn from S on several real-world datasets.

References

- A. Alanazi. Using machine learning for health-care challenges and opportunities. *Informatics in Medicine Unlocked*, 30:100924, 2022. ISSN 2352-9148. doi: <https://doi.org/10.1016/j.imu.2022.100924>. URL <https://www.sciencedirect.com/science/article/pii/S2352914822000739>.
- A. N. Angelopoulos and S. Bates. A gentle introduction to conformal prediction and distribution-free uncertainty quantification, 2022. URL <https://arxiv.org/abs/2107.07511>.
- S. Aziz, M. Dowling, H. Hammami, and A. Piepenbrink. Machine learning in finance: A topic modeling approach. *European Financial Management*, 28(3):744–770, 2022. doi: <https://doi.org/10.1111/eufm.12326>. URL <https://onlinelibrary.wiley.com/doi/abs/10.1111/eufm.12326>.
- B. Becker and R. Kohavi. Adult. UCI Machine Learning Repository, 1996. DOI: <https://doi.org/10.24432/C5XW20>.
- I. Ben-Gal. *Bayesian Networks*. John Wiley & Sons, Ltd, 2008. ISBN 9780470061572. doi: <https://doi.org/10.1002/9780470061572.eqr089>. URL <https://onlinelibrary.wiley.com/doi/abs/10.1002/9780470061572.eqr089>.
- S. Burkhardt, J. Siekiera, and S. Kramer. Semisupervised bayesian active learning for text classification. In *Bayesian Deep Learning Workshop at NeurIPS*, 2018.
- CDC. Behavioral risk factor surveillance system survey data (brfss), 2015. URL <https://www.cdc.gov/brfss/index.html>.
- L. Deng. The mnist database of handwritten digit images for machine learning research. *IEEE Signal Processing Magazine*, 29(6):141–142, 2012.
- L. L. Folgoc, V. Baltatzis, S. Desai, A. Devaraj, S. Ellis, O. E. M. Manzanera, A. Nair, H. Qiu, J. Schnabel, and B. Glocker. Is mc dropout bayesian?, 2021. URL <https://arxiv.org/abs/2110.04286>.
- J. Friedbaum, S. Adiga, and R. Tandon. Trustworthy actionable perturbations. In R. Salakhutdinov, Z. Kolter, K. Heller, A. Weller, N. Oliver, J. Scarlett, and F. Berkenkamp, editors, *Proceedings of the 41st International Conference on Machine Learning*, volume 235 of *Proceedings of Machine Learning Research*, pages 14006–14034. PMLR, 21–27 Jul 2024. URL <https://proceedings.mlr.press/v235/friedbaum24a.html>.
- C. Guo, G. Pleiss, Y. Sun, and K. Q. Weinberger. On calibration of modern neural networks. In D. Precup and Y. W. Teh, editors, *Proceedings of the 34th International Conference on Machine Learning*, volume 70 of *Proceedings of Machine Learning Research*, pages 1321–1330. PMLR, 06–11 Aug 2017. URL <https://proceedings.mlr.press/v70/guo17a.html>.
- R. Harper and J. Southern. A bayesian deep learning framework for end-to-end prediction of emotion from heartbeat. *IEEE transactions on affective computing*, 13(2):985–991, 2020.
- K. He, X. Zhang, S. Ren, and J. Sun. Deep residual learning for image recognition, 2015. URL <https://arxiv.org/abs/1512.03385>.
- H. Hofmann. Statlog (German Credit Data). UCI Machine Learning Repository, 1994. DOI: <https://doi.org/10.24432/C5NC77>.
- R. A. Horn and C. R. Johnson. *Positive definite matrices*, page 391–486. Cambridge University Press, 1985.
- E. Hüllermeier and W. Waegeman. Aleatoric and epistemic uncertainty in machine learning: An introduction to concepts and methods. *Machine learning*, 110(3):457–506, 2021.
- M. N. Murty and V. S. Devi. *Bayes Classifier*, pages 86–102. Springer London, London, 2011. ISBN 978-0-85729-495-1. doi: 10.1007/978-0-85729-495-1.4. URL <https://doi.org/10.1007/978-0-85729-495-1.4>.
- S. Nannapaneni, S. Mahadevan, and S. Rachuri. Performance evaluation of a manufacturing process under uncertainty using bayesian networks. *Journal of Cleaner Production*, 113:947–959, 2016. ISSN 0959-6526. doi: <https://doi.org/10.1016/j.jclepro.2015.12.003>. URL <https://www.sciencedirect.com/science/article/pii/S0959652615018144>.
- Y. Sale, P. Hofman, T. Löhr, L. Wimmer, T. Nagler, and E. Hüllermeier. Label-wise aleatoric and epistemic uncertainty quantification, 2024. URL <https://arxiv.org/abs/2406.02354>.
- K. Tumer and J. Ghosh. Bayes error rate estimation using classifier ensembles. *International Journal of Smart Engineering System Design*, 5(2):95–109, 2003. doi: 10.1080/10255810305042. URL <https://doi.org/10.1080/10255810305042>.
- L. F. Wightman. Lsac national longitudinal bar passage study. lsac research report series. 1998.

6 Appendix

The Appendix is organized as follows:

- 6.1 Broader Impact Statement
- 6.2 Proofs of Technical Results
 - 6.2.1 Proof of Theorem 2.6: The Properties of the Collision Matrix S
 - 6.2.2 Proofs from the Binary Classification Case Study
 - 6.2.3 Proof of Equation (10): The Formula for the Elements of the Gramian G
 - 6.2.4 Proof of Theorem 3.1: The Uniqueness of the Decomposition of the Gramian G
- 6.3 Algorithm and Experiment Details
 - 6.3.1 Gramian Based Algorithm Details and Complexity Analysis
 - 6.3.2 Baseline Algorithm Details and Complexity Analysis
 - 6.3.3 Synthetic Dataset Details
 - 6.3.4 Real Dataset Details
 - 6.3.5 Classifier Implementation Details
- 6.4 Additional Results: MNIST

6.1 Broader Impact Statement

Our work proposes a new statistic, the collision matrix, that describes the uncertainty inherent in a classification setting and provides an algorithm for estimating this collision matrix. This statistic provides a more fine-grained description of the uncertainty inherent to a dataset than previous methods and allows for prediction of the rates of particular classification types. Adoption of this statistic could help the practitioners of machine learning better understand the inherent limitations of prediction with specific datasets and help establish reasonable expectations. This metric would be of particular interest when costs involved with different types of classification errors vary significantly. The collision matrix could aid in understanding when more data or less specific predictions are required in order to achieve sufficiently trustworthy predictions.

6.2 Proofs of Technical Results

In all proofs we will assume that matrices are real valued $K \times K$ square matrices.

6.2.1 Proof of Theorem 2.6: The Properties of the Collision Matrix S

For this theorem we must prove that S is column stochastic, equation (6), and that S is doubly stochastic in the special case where $\boldsymbol{\pi} = (\frac{1}{K}, \frac{1}{K}, \dots, \frac{1}{K})$.

We begin by showing S is column stochastic. Clearly each element of S given by $\mathbb{E}_{\mathbf{x} \sim \mathcal{D}_j} \mathbb{P}(C = i | X = \mathbf{x})$ is positive, so we need to show that the entries of each

column of S sum to 1. For ease of notation we will refer to the k^{th} column of S as

$$\mathbf{s}(k) = \begin{pmatrix} \mathbb{E}_{\mathbf{x} \sim \mathcal{D}_k} \mathbb{P}(C = 1 | X = \mathbf{x}) \\ \mathbb{E}_{\mathbf{x} \sim \mathcal{D}_k} \mathbb{P}(C = 2 | X = \mathbf{x}) \\ \vdots \\ \mathbb{E}_{\mathbf{x} \sim \mathcal{D}_k} \mathbb{P}(C = K | X = \mathbf{x}) \end{pmatrix}. \quad (15)$$

We now show that the columns have the desired sum.

$$\begin{aligned} \sum_{j=1}^k \mathbf{s}_j(i) &= \sum_{j=1}^k \mathbb{E}_{\mathbf{x} \sim \mathcal{D}_i} \mathbb{P}(C = j | X = \mathbf{x}) \\ &= \mathbb{E}_{\mathbf{x} \sim \mathcal{D}_i} \sum_{j=1}^k \mathbb{P}(C = j | X = \mathbf{x}) \\ &= \mathbb{E}_{\mathbf{x} \sim \mathcal{D}_i} 1 \\ &= 1 \end{aligned}$$

Now we find the closed form expression (6) is equal to the elements of S as from Definition 2.3. Let $\mathcal{B}_\epsilon(\mathbf{x})$ be an ϵ ball in \mathbb{R}^d centered around \mathbf{x} .

$$\begin{aligned} \mathbb{P}(C = i | X = \mathbf{x}) &= \lim_{\epsilon \rightarrow 0} \mathbb{P}(C = i | X \in \mathcal{B}_\epsilon(\mathbf{x})) \\ &= \lim_{\epsilon \rightarrow 0} \frac{\mathbb{P}(X \in \mathcal{B}_\epsilon(\mathbf{x}) | C = i) \mathbb{P}(C = i)}{\mathbb{P}(X \in \mathcal{B}_\epsilon(\mathbf{x}))} \\ &= \lim_{\epsilon \rightarrow 0} \frac{\boldsymbol{\pi}_i \int_{\mathcal{B}_\epsilon(\mathbf{x})} f_i(\mathbf{z}) d\mathbf{z}}{\int_{\mathcal{B}_\epsilon(\mathbf{x})} \sum_{k=1}^K \boldsymbol{\pi}_k f_k(\mathbf{z}) d\mathbf{z}} \\ &= \frac{\boldsymbol{\pi}_i f_i(\mathbf{x})}{\sum_{k=1}^K \boldsymbol{\pi}_k f_k(\mathbf{x})} \end{aligned} \quad (16)$$

Applying an expectation to (16) we arrive at (6):

$$\mathbb{E}_{\mathbf{x} \sim \mathcal{D}_j} \mathbb{P}(C = i | X = \mathbf{x}) = \boldsymbol{\pi}_i \int_{\mathcal{X}} \frac{f_i(\mathbf{x}) f_j(\mathbf{x})}{\sum_{k=1}^K \boldsymbol{\pi}_k f_k(\mathbf{x})} d\mathbf{x}.$$

Finally, we note that when $\boldsymbol{\pi} = (\frac{1}{K}, \frac{1}{K}, \dots, \frac{1}{K})$, equation (6) simplifies to

$$S_{i,j} = \int_{\mathcal{X}} \frac{f_i(\mathbf{x}) f_j(\mathbf{x})}{\sum_{k=1}^K f_k(\mathbf{x})} d\mathbf{x}. \quad (17)$$

In this case $S_{i,j} = S_{j,i}$ and S is symmetric and, therefore, doubly stochastic. This completes the proof of this Theorem.

6.2.2 Proofs for the Binary Classification Case Study

We must prove that when $K = 2$ and $\boldsymbol{\pi} = (1/2, 1/2)$, we have $S_{1,2} \in [0, 1/2]$ with a minimum of 0 when \mathcal{D}_1 and \mathcal{D}_2 have disjoint support and a maximum of 1 when $\mathcal{D}_1 = \mathcal{D}_2$.

We begin with applying $K = 2$ and $\pi = (1/2, 1/2)$ to (6) to arrive at

$$S_{1,2} = \int_{\mathcal{X}} \frac{f_{\mathcal{D}_1}(\mathbf{x})f_{\mathcal{D}_2}(\mathbf{x})}{f_{\mathcal{D}_1}(\mathbf{x}) + f_{\mathcal{D}_2}(\mathbf{x})} d\mathbf{x}. \quad (18)$$

Clearly, each term in (18) is non-negative and the entire integral must be lower bounded by 0. Furthermore, when \mathcal{D}_1 and \mathcal{D}_2 have disjoint support the numerator is always 0, so $S_{1,2} = \int_{\mathcal{X}} 0 d\mathbf{x} = 0$.

To prove the upper bound we recall that the arithmetic mean (AM) and harmonic mean (HM) inequality states that $HM(a, b) \leq AM(a, b)$. Using this inequality, we arrive at

$$\frac{2f_{\mathcal{D}_1}(\mathbf{x})f_{\mathcal{D}_2}(\mathbf{x})}{f_{\mathcal{D}_1}(\mathbf{x}) + f_{\mathcal{D}_2}(\mathbf{x})} \leq \frac{f_{\mathcal{D}_1}(\mathbf{x}) + f_{\mathcal{D}_2}(\mathbf{x})}{2}. \quad (19)$$

Substituting (19) in (18), we have that

$$\begin{aligned} S_{1,2} &\leq \int_{\mathcal{X}} \frac{f_{\mathcal{D}_1}(\mathbf{x}) + f_{\mathcal{D}_2}(\mathbf{x})}{4} d\mathbf{x} \\ &= \frac{1}{4} \left(\int_{\mathcal{X}} f_{\mathcal{D}_1}(\mathbf{x}) d\mathbf{x} + \int_{\mathcal{X}} f_{\mathcal{D}_2}(\mathbf{x}) d\mathbf{x} \right) = \frac{1}{2} \end{aligned} \quad (20)$$

We now show this upper bound is obtained when the distributions are identical by substituting $f_{\mathcal{D}_1}(\mathbf{x}) = f_{\mathcal{D}_2}(\mathbf{x})$ into (18) to get

$$\begin{aligned} S_{1,2} &= \int_{\mathcal{X}} \frac{f_{\mathcal{D}_1}(\mathbf{x})f_{\mathcal{D}_1}(\mathbf{x})}{f_{\mathcal{D}_1}(\mathbf{x}) + f_{\mathcal{D}_1}(\mathbf{x})} d\mathbf{x} \\ &= \frac{1}{2} \int_{\mathcal{X}} f_{\mathcal{D}_1}(\mathbf{x}) d\mathbf{x} = \frac{1}{2}. \end{aligned} \quad (21)$$

6.2.3 Proof of Equation (10): The Formula for the Elements of the Gramian G

To prove (10), we will use the notation from (15). We may now expand the element of $G = S^T S$ as

$$\begin{aligned} G_{i,j} &= \mathbf{s}(i)^T \mathbf{s}(j) \\ &= \sum_{i=k}^K \mathbb{E}_{\mathbf{x} \sim \mathcal{D}_i} [\mathbb{P}(c = k | \mathbf{x})] \mathbb{E}_{\tilde{\mathbf{x}} \sim \mathcal{D}_j} [\mathbb{P}(\tilde{c} = k | \tilde{\mathbf{x}})] \\ &= \mathbb{E}_{\mathbf{x} \sim \mathcal{D}_i} \left[\mathbb{E}_{\tilde{\mathbf{x}} \sim \mathcal{D}_j} \left[\sum_{k=1}^K \mathbb{P}(c = k | \mathbf{x}) \mathbb{P}(\tilde{c} = k | \tilde{\mathbf{x}}) \right] \right] \\ &= \mathbb{E}_{\mathbf{x} \sim \mathcal{D}_i} \left[\mathbb{E}_{\tilde{\mathbf{x}} \sim \mathcal{D}_j} [\mathbb{P}(c = \tilde{c} | \mathbf{x}, \tilde{\mathbf{x}})] \right]. \end{aligned}$$

The last equality above takes advantage of the fact that \mathbf{x} and $\tilde{\mathbf{x}}$ are drawn independently from \mathcal{D}_i and \mathcal{D}_j respectively. Recall that when $\pi = (1/K, 1/K, \dots, 1/K)$, S is doubly stochastic (and consequently so is S^T). This implies $S^T S = G$ is also doubly stochastic.

6.2.4 Proof of Theorem 3.1: The Uniqueness of the Decomposition of the Gramian G

This Theorem states that if G is the Gramian Matrix of an invertible collision matrix S and stochastic matrix L satisfies $L^T L = G$, there exists a orthogonal matrix Q such that $L = QS$. We take advantage of two lemmas to prove this Theorem.

Lemma 6.1 *For any two real square matrices A and B , $A^T A = B^T B$ if and only if there exists an orthogonal matrix Q , such that $A = QB$.*

Proof: We begin with $A = QB \implies A^T A = B^T B$.

$$\begin{aligned} A^T A &= (QB)^T QB \\ &= B^T Q^T QB \\ &= B^T B \end{aligned}$$

We now prove $A^T A = B^T B \implies A = QB$. This proof will take advantage of the *Singular Value Decomposition* (SVD) and the fact that symmetric positive semi-definite matrices have a unique positive semi-definite square root (see Horn and Johnson (1985)).

We will write the SVDs of A and B as

$$\begin{aligned} A &= U_A \Sigma_A V_A^T \\ B &= U_B \Sigma_B V_B^T, \end{aligned}$$

where U_A , U_B , V_A , and V_B are orthogonal matrices and Σ_A and Σ_B are diagonal matrices with non-negative entries. Note that

$$\begin{aligned} A^T A &= V_A \Sigma_A \Sigma_A V_A^T \\ &= (V_A \Sigma_A V_A^T)(V_A \Sigma_A V_A^T). \end{aligned}$$

We note $A^T A$ is positive semi-definite ($\mathbf{x}^T A^T A \mathbf{x} = \|\mathbf{A}\mathbf{x}\|^2 \geq 0$) and $V_A \Sigma_A V_A^T$ is positive semi-definite (because it is similar Σ_A which is diagonal with non-negative entries). This means that $V_A \Sigma_A V_A^T$ is the unique positive semi-definite square root of $A^T A$. We can similarly prove that $V_B \Sigma_B V_B^T$ is the unique positive semi-definite square root of $B^T B$. Because $A^T A = B^T B$ and these square roots are unique, we have that

$$V_A \Sigma_A V_A^T = V_B \Sigma_B V_B^T. \quad (22)$$

Now consider,

$$A = U_A \Sigma_A V_A^T \quad (23)$$

$$= U_A V_A^T V_A \Sigma_A V_A^T \quad (24)$$

$$= U_A V_A^T V_B \Sigma_B V_B^T \quad (25)$$

$$= U_A V_A^T V_B U_B^T U_B \Sigma_B V_B^T \quad (26)$$

$$= U_A V_A^T V_B U_B^T B, \quad (27)$$

where (24) and (26) come from multiplying by the identity ($I = V_A^T V_A = U_B^T U_B$), and (25) comes from applying (22). Finally, we note that

$$Q = U_A V_A^T V_B U_B^T,$$

is orthogonal because it is the product of orthogonal matrices. This gives us

$$A = QB.$$

Lemma 6.2 *Any matrix Q that is both orthogonal and stochastic is a permutation matrix.*

Proof: We first note that one way to characterize permutation matrices is a stochastic matrix whose elements are all either 1 or 0. This result is true for either row or column stochastic matrices but we will use column stochasticity in our proof.

Because Q is orthogonal we have $Q^T Q = I$. Extracting the calculations for the finding for the diagonal entries of this product we see

$$\sum_{k=1}^K Q_{i,k} Q_{k,i} = 1, \quad (28)$$

for all $1 \leq i \leq K$. Because Q is column stochastic we also have

$$\sum_{k=1}^K Q_{k,i} = 1. \quad (29)$$

for all $1 \leq i \leq K$. By subtracting (28) from (29) we get

$$\begin{aligned} \sum_{k=1}^K Q_{k,i} - \sum_{k=1}^K Q_{i,k} Q_{k,i} &= 1 - 1 \\ \sum_{k=1}^K Q_{k,i} (1 - Q_{k,i}) &= 0. \end{aligned} \quad (30)$$

Note, because Q is stochastic $0 \leq Q_{k,i} \leq 1$ and every term on the sum in (30) is non-negative. Then the only way for (30) to be satisfied is if $Q_{k,i}(1 - Q_{k,i}) = 0$ which implies $Q_{k,i} = 0$ or $Q_{k,i} = 1$. This is true for all $i, k \in \{1, 2, \dots, K\}$, so Q is a stochastic matrix whose elements are all either 1 or 0. This means that Q is a permutation matrix by definition.

Proof of Theorem 3.1: Let $G = S^T S$ be the Gramian Matrix of an invertible stochastic matrix S . Then a stochastic matrix L satisfies $L^T L = G$ if and only if $L = PS$ for some permutation matrix P .

Proof: By lemma 6.1 and the fact that $L^T L = S^T S$ we have that there exists a orthogonal matrix Q such that $L = QS$. For the following calculations we will use 1

to refer to the K length column vector containing all values 1.

$$\begin{aligned} L^T &= S^T Q^T \\ L^T \mathbf{1} &= S^T Q^T \mathbf{1} \\ \mathbf{1} &= S^T (Q^T \mathbf{1}). \end{aligned} \quad (31)$$

Because S is invertible S^T is invertible and there is a unique solution to $S^T \mathbf{v} = \mathbf{1}$. Because S is column stochastic $S^T \mathbf{1} = \mathbf{1}$. Then (31) is only true when $Q^T \mathbf{1} = \mathbf{1}$ and Q is column stochastic. Then by Lemma 6.2 Q must be a permutation matrix.

Algorithm 2 Collision Matrix Estimation via Pair-wise Contrast

Input: $\mathcal{T} = \{\mathcal{T}_1, \mathcal{T}_2, \dots, \mathcal{T}_K\}$ partitioned training data and learning rate η .

Step 1: Estimating Gramian Matrix G

Train binary contrast verifier V on the difference training data $\mathcal{T}_{\text{difference}}$ (defined in (11)).

for $\mathbf{x} \in \mathcal{T}_i$ **do**

for $\tilde{\mathbf{x}} \in \mathcal{T}_j$ **do**

 Compute $G_{i,j} = \frac{1}{|\mathcal{T}_i|} \sum_{\mathbf{x} \in \mathcal{T}_i} \frac{1}{|\mathcal{T}_j|} \sum_{\tilde{\mathbf{x}} \in \mathcal{T}_j} V(\mathbf{x}, \tilde{\mathbf{x}})$

end for

end for

Step 2: Estimating Collision Matrix S

(a) **Initialize:** $S = I$ (or any diagonally dominant matrix)

(b) **Iterative approach:**

while $\|S^T S - \hat{G}\|_F > \gamma$ **do**

$S = S - \eta \nabla_S \|\hat{S}^T \hat{S} - \hat{G}\|_F$

$- \eta \nabla_S \left(\lambda \|\hat{S}^T \mathbf{1} - \mathbf{1}\|_1 - \sum_{i=1}^K \sum_{j=1}^K \min\{\hat{S}_{i,j}, 0\} \right)$

end while

return S

6.3 Algorithm and Experiment Details

6.3.1 Gramian Based Algorithm Details and Complexity Analysis

Algorithm 2 provides a detailed implementation of the meta-algorithm found in the paper (Algorithm 1).

Complexity: Algorithm 2 proposes estimating S in two steps: (a) compute the Gramian G and (b) recover S from G . We will compare the tasks involved in each of these steps (recall K is the number of classes and n is the number of points in the training data):

- a) We first train the pairwise classifier V , then compute an empirical estimate for each of the K^2 elements of G by calculating the average of a series of outputs from V . These empirical estimates require n^2 evaluations of V , one evaluation for each element of $\mathcal{T}_{\text{difference}}$. In practice, however, we found it was equally effective to pick a number m of randomly selected elements to use in each average. This strategy requires only mK^2 evaluations of V .
- b) We run a K^2 dimensional gradient descent algorithm on optimization problem (14) from the paper to find the our estimated collision matrix \hat{S} .

In practice the training of V dominates all other tasks as it involves optimizing across all the parameters of V (which includes far more than K^2 values) over the difference training data (which has n^2 elements). PAC-bounds from Friedbaum et al. (2024) show that V is learnable, however, do not indicate how complex the model V should be nor how long it will take to train. In our experiments the pairwise classifier V trains in a similar amount of time to a regular classifier M on the same data. One important note is: if there are n points in the training data, there are n^2 pairs of data points to train V (see equation (11)). Thus our method can be applied even to settings with a limited number of points in the training data.

6.3.2 Details of Baseline Algorithms and Complexity

The algorithm we use as a baseline to test our Gramian based algorithm (Algorithm 2) against is described in Algorithm 3.

Algorithm 3 Baseline Collision Matrix Estimation Algorithm

Input: $\mathcal{T} = \{\mathcal{T}_1, \mathcal{T}_2, \dots, \mathcal{T}_K\}$ partitioned training data and learning rate η .

Train classifier M on the training data \mathcal{T} to estimate posterior class probability distributions.

for $\mathbf{k} \in \{1, 2, \dots, k\}$ **do**

Compute $\mathbf{s}_k = \frac{1}{|\mathcal{T}_k|} \sum_{\mathbf{x} \in \mathcal{T}_k} C(\mathbf{x})$

end for

return S

Complexity: Algorithm 3 requires us to train a model M which estimates class posterior probabilities (not just achieve high accuracy) and then evaluate M n times, once for each element of the training data \mathcal{T} . This is dominated by the time required to train the model M . We used three techniques to train a classifier to estimate class posterior probabilities all

based on Neural Networks:

Calibrated Classifier (Guo et al., 2017): We use temperature scaling to create a calibrated classifier, motivated by Guo et al. (2017) who found this to be the most effective method for calibration. This method involves splitting the data set into a training and validation set. A classifier is then trained to maximize accuracy on the training set. We then test a variety of temperature scale parameters T . This involves dividing the logits of the model (output immediately before the soft-max layer) by T and then finding the *Expected Calibration Error* (ECE) over the validation set. The value for T^* that leads to the lowest ECE on the validation data is then selected and in all future evaluations of the classifier logits are divided by T^* before the soft-max layer. This baseline technique has the least computational expense and only requires the training of a classifier using typical methods and then the calculation of the ECE for a variety of values T . Notably all evaluations of the calibrated classifier are no more computationally complex than evaluations of a regular classifier.

Monte Carlo Dropout (Folgotc et al., 2021): This method involves training a classifier that includes dropout layers to maximize accuracy on the training data. During test time we leave the dropout layers functional (contrary to typical usage) which adds randomness to the outputs of the classifier. During inference we run the input through the network h times where h is a parameter which must be selected. The final output is then taken as the average of all h outputs. This techniques adds very little complexity to training the algorithm, but does increase the inference costs by a factor of h .

Bayesian Neural Network (BNN) (Ben-Gal, 2008): In this method a prior probability distribution is assigned to each parameter of the neural network. The training data is then used to shift the prior distribution into posterior distributions that better fit the data. During evaluation we sample all network parameters from the posterior distributions h times. We then evaluate the input on each of the h networks and average the results to create the final output of the BNN. This increases inference costs by a factor of h compared to a regular neural network, and as noted in Section 4 Scenario 3, requires much longer training times.

6.3.3 Synthetic Dataset Details

We elaborate on the dataset generation process for the experiments on synthetic data. In all Gaussian distributions the covariance matrix was set to the identity matrix I and the means μ_k where adjusted to change the amount of overlap/uncertainty in the system. We use $\mathbf{1}$ to represent a vector with all elements equal to

Synthetic Data Model Hyper-Parameters

	Architecture	Activation Function	Objective Function	Evaluations Averaged per Prediction	Additional Parameters
Verifier	Six fully connected linear layers of 128 nodes each	ReLU	Cross-Entropy Loss	1	NA
Calibrated Classifier	Six fully connected linear layers of 128 nodes each	ReLU	Cross-Entropy Loss	1	Temperature Scales Tested $\{0.1, 0.2, \dots, 1\} \cup \{1, 2, \dots, 10\}$
MC Dropout Network	Six fully connected linear layers of 128 nodes each	ReLU	Cross-Entropy Loss	100	10% chance of dropout
Bayesian Network	Six fully connected linear layers of 128 nodes each	ReLU	Cross-Entropy Loss + KL-Divergence to Priors	100	Prior Distributions: $\mathcal{N}(\mu = 0, \sigma = 0.1)$ Weight on KL-Divergence: 0.01

Figure 6: Explanation of the hyper-parameters used to create the verifier V and the various models M used in the baseline approaches on synthetic datasets.

1 where the dimension may be inferred by context.

Scenario A: The dimension was set at $d = 4$, 250 points were sampled from each class and the number of classes was varied. We used the following means for each class:

- $K = 3$ classes: $\mu_1 = 0.25 \cdot \mathbf{1}$, $\mu_2 = -0.25 \cdot \mathbf{1}$, and $\mu_3 = 1.25 \cdot \mathbf{1}$
- $K = 4$ classes: $\mu_1 = -0.25 \cdot \mathbf{1}$, $\mu_2 = 0.25 \cdot \mathbf{1}$, $\mu_3 = 0.75 \cdot \mathbf{1}$, and $\mu_4 = 2.5 \cdot \mathbf{1}$
- $K = 5$ classes: $\mu_1 = -0.25 \cdot \mathbf{1}$, $\mu_2 = 0.25 \cdot \mathbf{1}$, $\mu_3 = 0.75 \cdot \mathbf{1}$, $\mu_4 = 2.5 \cdot \mathbf{1}$, and $\mu_5 = -1 \cdot \mathbf{1}$

Scenario B: The dimensionality was fixed at $d = 20$ and all experiments used $K = 5$ classes and 10,000 points sampled from each class. The orientation of the position of the means were selected as $\mu_1 = -3\beta \cdot \mathbf{1}$, $\mu_2 = -\beta \cdot \mathbf{1}$, $\mu_3 = \beta \cdot \mathbf{1}$, $\mu_4 = 5\beta \cdot \mathbf{1}$, and $\mu_5 = 10\beta \cdot \mathbf{1}$. The value of β was adjusted to control the amount of overlap between sets which corresponds to the amount of classification uncertainty. The most overlap/uncertainty used $\beta = 0.15$, the intermediate overlap/uncertainty used $\beta = 0.25$ and the least overlap/uncertainty used $\beta = 0.35$.

Scenario C: This used the same dataset as the most overlap setting from Scenario B.

In these synthetic datasets we have access to the pdfs of the data from each class (the \mathcal{D}_k s) and we can use equation (6) to calculate S directly. We estimate the integral using Monte Carlo integration. We can also find the true posterior class probability distribution of any data point \mathbf{x} using

$$y_i(\mathbf{x}) = \frac{\pi_i f_i(\mathbf{x})}{\sum_{k=1}^K \pi_k f_k(\mathbf{x})}, \quad (32)$$

where f_k is the pdf corresponding to class k . This allows us to implement the Bayes optimal classifier and find the BER, again using Monte Carlo integration.

6.3.4 Real Dataset Details

The four real world datasets used in our experiments represented different setting in which there is a clear the possibility of class collisions, indicating the presence of aleatoric uncertainty.

German Credit Dataset: (Hofmann, 1994) This commonly used data set contains information on 1,000 loan applications in Germany labelled by their credit risk. The opportunity for class collisions in this dataset comes from the fact that many factors not included on a loan application can affect whether the individual pays off the loan. For example, suppose two individuals submit identical loan applications, but after the loan is granted the first individual loses his job and has a car accident resulting in unforeseen medical expenses. This could cause the first individual to default on the loan, whereas, the second individual (who did not experience these unfortunate events) pays off the loan resulting in a class collision.

Adult Income Prediction Dataset: (Becker and Kohavi, 1996) This widely used data set contains information from the 1994 U.S. census, with individuals labelled by whether their annual income was over \$50,000 (\sim \$100,000 in 2024 adjusted for inflation). In this dataset, two people could have identical feature vectors well differing in key ways: for example having majored in very different fields in school or living in totally different parts of the country. Considering the wide variability between individuals with identical feature vectors we would expect class collisions to be very possible.

Law School Success Prediction Dataset: (Wightman,

1998) This data set contains demographic information and academic records (consisting of undergraduate GPA, LSAT score, and first year law school grades) for over 20,000 law school students labelled by whether or not a student passed the BAR exam. Here it is very possible that two students with identical features could differ in whether they passed the BAR based off of how much they studied and even sheer luck in guessing answers. This means that class collisions are possible and aleatoric uncertainty is present.

Diabetes Prediction Dataset: (CDC, 2015) This data set contains information on the demographics, health conditions and health habits of 250,000 individuals labelled by whether an individual is diabetic extracted from the Behavioral Risk Factor Surveillance System (BRFSS), a health-related telephone survey that is collected annually by the CDC. The medical field is notorious for individuals with the same health habits having different medical outcomes indicating that class collisions are possible in this dataset.

6.3.5 Classifier Implementation Details

Our code is available online². All experiments were run using an NVIDIA RTX 4060 GPU. We used the PyTorch³ python package to create the classifiers for all experiments.

Synthetic Data Experiments: For the experiments on synthetic Gaussian data both classifiers M and verifiers V , we use feedforward fully connected neural networks with 6 hidden layers and layer each containing 128 nodes with ReLU activation functions. We note however, that the number of inputs and outputs does differ between the M and V (M has a d dimensional input and k dimensional output, whereas, V has a $2d$ dimensional input and a 2 dimensional output). On synthetic data all models were trained to minimize the cross-entropy loss for a total of 500 epochs, where an epoch involves showing the model n data points. (We do not consider an epoch for the verifier V to involve n^2 data points even though there are n^2 points in the training data. In this way training the verifier V or a classifier M for one epoch takes approximately the same amount of time.)

We next describe the specific modifications made to this architecture for implementing MC Dropout and BNN baselines.

MC Dropout: For this method we added dropout likelihoods of 10% to each hidden layer. During evaluation we averaged $h = 100$ outputs for the final prediction.

BNN: For this method we used the torchbnn⁴ add-

²<https://anonymous.4open.science/r/Classification-Uncertainty9055/Readme>

³<https://pytorch.org>

⁴<https://pypi.org/project/torchbnn/>

Real World Data Model Hyper-Parameters

Dataset	German Credit	Adult Income, Law School Success & Diabetes Prediction
Number of Layers	5	5
Nodes per Layer	120	60
Dropout Chance	20%	0%

Figure 7: Explanation of the hyper-parameters used to create the verifier V on real world datasets.

on for PyTorch. We set the prior distribution on all weights to be normal distributions with hyper-parameters as $\mu = 0$ and $\sigma = 0.1$. We trained to minimize the cross entropy loss over the training data plus 0.01 times the KL-divergence between the prior and the posterior distributions on the network weights. Finally, during evaluation we averaged $h = 100$ samples from the posterior distributions.

See the table in Figure 6 for a summary of these parameters.

Real Data Experiments We again used fully connected feedforward neural networks with RELU activation functions. Each network used 5 hidden layers (each containing 60 nodes) except for the classifier on the German Credit data which used hidden layers with 120 nodes and 20% dropout chance on each hidden layer (during training only). This change was motivated by the fact that we wished to achieve accuracy on par with common tree based classifiers (random forests and histogram boosted trees). This was not possible on the German Credit data without augmenting its architecture. We used an 80 – 10 – 10 train-validate-test data split and stopped training when accuracy on the validation data ceased to increase. See the table in Figure 7 for a summary of these parameters.

6.4 Additional Results: MNIST

We also used Algorithm 2 to estimate the collision matrix for the MNIST dataset (Deng, 2012) (seen in Figure 8). This image classification dataset contains black and white scans of handwritten digits where the label corresponds to the number that the writer intended to draw. Many image classification datasets have no possibility for class collision (no aleatoric uncertainty) and are not good candidates for estimating the collision matrix S . This is because the subject of an image will be the same each time the image is viewed. MNIST, however, does allow for collisions because the label represents the number the writer intended to draw (the

Collision Matrix S for The MNIST Dataset

0.983	0.001	0.002	0.001	0.002	0.002	0.005	0.001	0.002	0.001
0.001	0.98	0.003	0.001	0.002	0.001	0.002	0.007	0.002	0.001
0.002	0.003	0.97	0.005	0.002	0.001	0.002	0.007	0.008	0.001
0.001	0.001	0.005	0.971	0	0.014	0.001	0.001	0.005	0.002
0.002	0.002	0.002	0	0.95	0.001	0.004	0.004	0.007	0.028
0.002	0.001	0.001	0.014	0.001	0.962	0.009	0.001	0.005	0.006
0.005	0.002	0.002	0.001	0.004	0.009	0.972	0	0.004	0
0.001	0.007	0.007	0.001	0.004	0.001	0	0.969	0.002	0.007
0.002	0.002	0.008	0.005	0.007	0.005	0.004	0.002	0.961	0.004
0.001	0.001	0.001	0.002	0.028	0.006	0	0.007	0.004	0.95

Figure 8: Collision matrix S for the MNIST (Deng, 2012) dataset found using Algorithm 2. The largest off diagonal entries are highlighted representing the class collisions between the digits 4 and 9 and also between digits 3 and 5. This indicates that there is a small amount of inherent uncertainty in these pairs of digits: it is not always possible to tell what digit the writer intended to make based off of what they actually drew.

Possible Class Collision in MNIST

MNIST Image				
Intended Digit	9	4	3	5
Other Possible Interpretation	4	9	5	3

Figure 9: Four examples of images in MNIST that could result in class collisions: if these exact same images here drawn on a different occasion it is possible (even likely) that writer intended to draw a different number than on the first occasion.

writer’s intent) and it is possible that the same drawing could be made multiple times even though the writer’s intended to draw distinct numbers. For examples of this see Figure 9, which contains 4 images from the MNIST dataset the could reasonably be interpreted as multiple digits.

Implementation Details: To create the verifier V for this dataset we used a the ResNet 18 architecture (He et al., 2015) with two input channels. To feed two inputs at a time into the classifier, we put each of the images (which only have one channel because they are black an white) into one of the two input channels to the classifier.

Results: Our estimate of the collision matrix S is found in Figure 8. Most off-diagonal entries were very small (less than 0.01) indicating very low likelihood of class collisions and low uncertainty. For the digit pairs 4 & 9 as well as 3 & 5, we did find collision probabilities above 0.01, indicating these digit pairs had the great-

est inherent uncertainty. Specifically, the fact that $S_{4,9} = 0.028$ indicates that if the same exact hand drawn digit that was originally intended to be a 4 is seen again, then there is a 2.8% chance that the second time it is observed it was meant to be a 9. These particular digit pairs are easily confused in the handwriting of some individuals (as shown in Figure 9), and the fact that the S matrix showed the highest uncertainty for these pairs indicates that Algorithm 1 is effective.